First-principles study of the thermal transport properties of superconducting NbN

Sen Liu[1a], Xiaoliang Zhang[1b*] and Dawei Tang[1c*]

[1] Key Laboratory of Ocean Energy Utilization and Energy Conservation of Ministry of Education, School of Energy and Power Engineering, Dalian University of Technology, Dalian 116024, China

Abstract: We investigate the thermal transport properties of NbN by considering three-phonon scattering (3ph), four-phonon scattering (4ph), electron-phonon (ep) scattering, and isotope (iso) scattering. By considering 4ph scattering, we find that 4ph scattering has less effect on the lattice thermal conductivity (κ_{ph}) within 3-9 THz, while ep scattering has a greater effect on κ_{ph} which is close to 3ph scattering in this frequency range. When the pressure is increased to 15 GPa, the κ_{ph} by 148%, which is due to the decrease of the scattering phase space resulting in an increase of phonon relaxation time. We find that the κ_{ph} of NbN is close to 100 W/mK, which is a potential high thermal conductivity material.

1. Introduction

Materials formed from 4d and 5d transition metals and light elements have received more attention. With the high electron density in transition metals and the strong bonds, such materials can resist elastic and plastic deformation, such as NbN. The material is a superconductor and can be used in resistance-free electrical transmission, nuclear magnetic resonance, and superconducting quantum computers. Moreover, TaN has been shown to have ultra-high lattice thermal conductivity (κ_{ph})[1], which is comparable to BAs. The dispersion curve of NbN is similar to that of TaN, and Nb is the same group element as Ta, so we predict that NbN should also have a high κ_{ph}.

In the different configurations of NbN, the critical temperature of the NaCl-phase is high but unstable, and the pressure required for the synthesis of the CsCl-phase is too high, reaching 290 GPa[2]. In contrast, the WC-phase has a stable structure at normal pressure. Although it has a small electron-phonon coupling (epc) and critical temperature, it has a similar lattice constant and structure to GaN which has better topological properties and can form a semiconductor-superconductor heterojunction[3]. At present, the research on NbN mainly focuses on its electrical, elastic, mechanical, and other properties, and there is a lack of thermal transport properties. Therefore, in this paper, the κ_{ph} of the NbN WC-phase is calculated by VASP[4] and ShengBTE[5], and the epc is calculated by QE[6] and EPW[7]. In addition, TDEP[8] is used to calculate the κ of the material. For the κ_{ph}, we consider a complete mechanism of phonon scattering to provide a comprehensive and profound understanding of the thermal transport properties of NbN. This is of significance for the thermal management of equipment such as energy management devices and superconducting devices.

2. Computational methods

We employ the first-principles calculations using VASP on the basic of density functional theory. The electron-ion interaction is described by the plane wave pseudopotential[9]. The PBE is chosen as the exchange-correlation functional. The energy convergence value is 1×10^{-8} eV. The shape and volume of the unit cell are sufficiently optimized.

The supercells of 5×5×5 and the k points of 1×1×1 is constructed to calculate the second-order force constant (harmonic properties); Supercells of 4×4×4 and k-points of 1×1×1 is used to calculate the third-order force constant (anharmonic properties). Use EPW to calculate ep coupling, starting from coarse k-grids 8×8×8 and q-grids 4×4×4, interpolated into dense k-grids 60×60×60 and q-grids 30×30×30. Finally, the ep coupling constant converged, and the value was 0.11.

The variation of lattice thermal conductivity(κ_{ph}) with cutoff distance and Q grids is shown in Fig. 1, and our calculation results show that the κ_{ph} has converged at the 9th nearest neighbor, which corresponds to the normalized force constant close to 0. We choose the 2nd nearest neighbor for the fourth-order force constant. When only considering 3ph scattering, our test results show that the κ converges at 20×20×20 Q grid; When considering both 3ph and 4ph scattering, we find that the result of 12×12×12 and the result of 14×14×14 is not more than 6%, we choose the Q grid as 12×12×12 for the measurement of computational resources and the accuracy of the results.

[a]L22010085@mail.dlut.edu.cn, [b*]zhangxiaoliang@dlut.edu.cn, [c*]dwtang@dlut.edu.cn

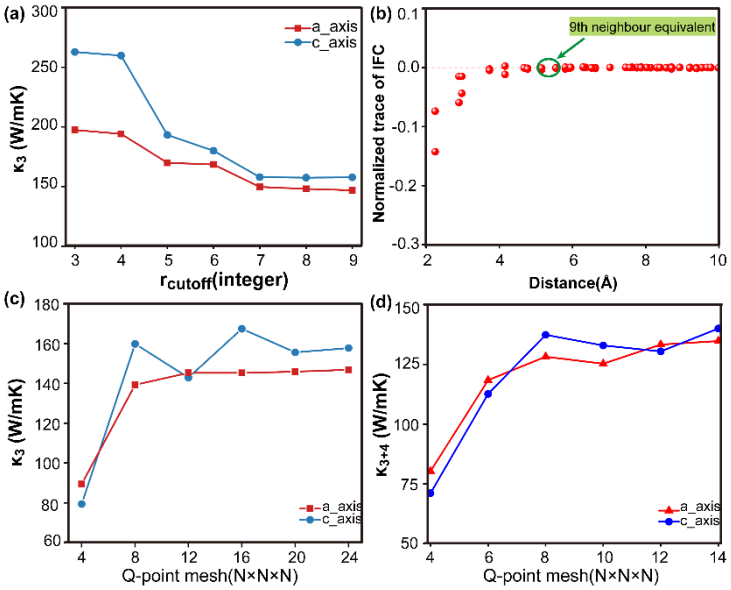

Fig. 1 (a) The convergence of κ_{ph} vs cutoff distance at 300 K; (b) normalized force constant; (c) the convergence of κ_{ph} considering 3ph scattering vs Q grid; (d) the convergence of κ_{ph} considering 3ph and 4ph scattering vs Q grid.

3. Lattice thermal conductivity (κ_{ph}) analysis

3.1 Phonon dispersion relationship and electronic band structure

The NbN structure, as shown in Fig. 2(a), is a hexagonal crystal system. Its lattice constant is a = 2.976Å, c = 2.9Å, because the pseudopotential used in the calculation is PBE, so the lattice constant will be larger than the experimental value, but it is consistent with the previous literature. The dispersion relationship and band structure are shown in Fig. 2(c), and the dispersion relationship without imaginary frequency indicates the stability of its structure. Since NbN contains two atoms, the dispersion relationship has six branches (3 acoustics + 3 optics). In the dispersion relationship, the color of the curve changes from blue to red, representing the epc from weak to strong. It can be observed that the epc is intense at high frequencies, and the epc constant is 0.11. The phonon density of states (DOS) shows that low-frequency phonons are mainly contributed by heavy atoms Nb, and the phonons are contributed by N atoms in high frequencies. And there is a band gap between the acoustic and optical branches. Fig. 2(d) shows the band structure and electron DOS of NbN, and the small DOS near the Fermi level is one of the reasons for the weak epc of NbN, and from the perspective of the electron DOS near the Fermi level, the material is mainly contributed by Nb atoms. In addition, we fit the energy bands through Wannier. Fig. 2(b) shows the band fitting plot, and good agreement shows the accuracy of our calculation results and the correctness of the projection orbital selection.

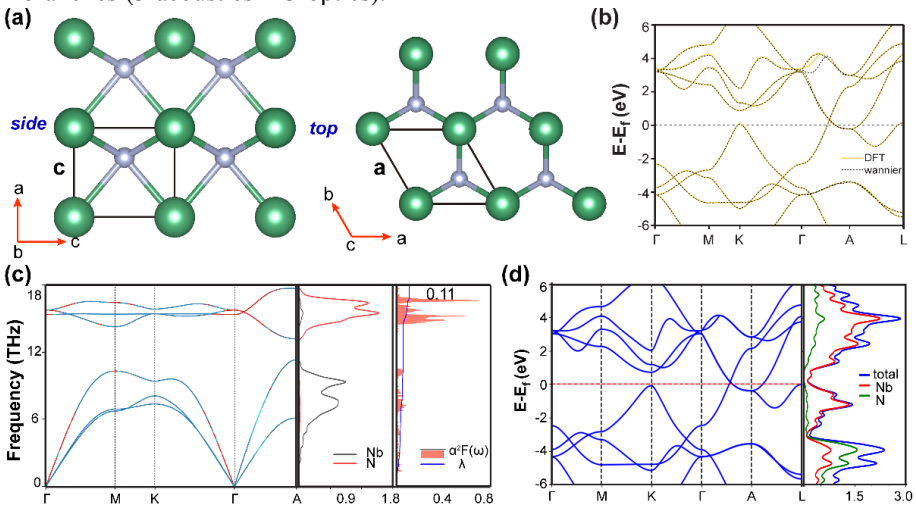

Fig. 2 (a) Side and top view of the NbN structure (green atoms represent Nb, silver atoms represent N); (b) DFT and Wannier band structure comparison; (c) phonon dispersion, phonon DOS and ep coupling; (d) band structures and electron DOS.

3.2 Lattice thermal conductivity (κ_{ph})

κ_{ph} is calculated as the sum of all phonon modes' contribution, which can be calculated from lattice dynamics theory, as follows:

$$\kappa=\frac{1}{3}\sum_{qv} C_{qv} v_{qv}^2 \tau_{qv} \quad (1)$$

where C_{qv} is specific heat capacity, v_{qv} and τ_{qv} are group velocity and phonon relaxation time. Among them, the calculation of phonon relaxation time is the most critical. Based on Matthiessen's rule, we use the iterative solution of the phonon Boltzmann equation (BTE) to calculate the total phonon relaxation time considering ep scattering:

$$\frac{1}{\tau_{qv}}=\frac{1}{\tau_{qv}^{3ph}}+\frac{1}{\tau_{qv}^{4ph}}+\frac{1}{\tau_{qv}^{ph-iso}}+\frac{1}{\tau_{qv}^{ph-el}} \quad (2)$$

where $1/\tau_{qv}^{3ph}$ is intrinsic 3ph scattering rate, which $1/\tau_{qv}^{4ph}$ is 4ph scattering rate. $1/\tau_{qv}^{ph-iso}$ and $1/\tau_{qv}^{ph-el}$ are iso scattering rate and ep scattering rate.

Fig. 3(a) shows the trend of κ_{ph} with temperature, in accordance with $\kappa_L \propto T^{-1}$. The matched calculation results of ShengBTE and TDEP indicate the accuracy of our results. Fig. 3(b) shows that the κ_{ph} is 146 W/mK when the scattering processes are 3ph and iso scattering, but after considering 4ph scattering and ep scattering, the κ_{ph} becomes 99 W/mK, a decrease of 32%, indicating the importance of 4ph scattering and ep scattering. Considering the weak anisotropy of NbN, Fig. 3(c) and (d) shows the differential of κ_{ph} to frequencies along the *a* and *c* axes. The contribution to κ_{ph} mainly comes from frequencies in 3-9 THz, so the κ_{ph} is mainly contributed by acoustic phonons.

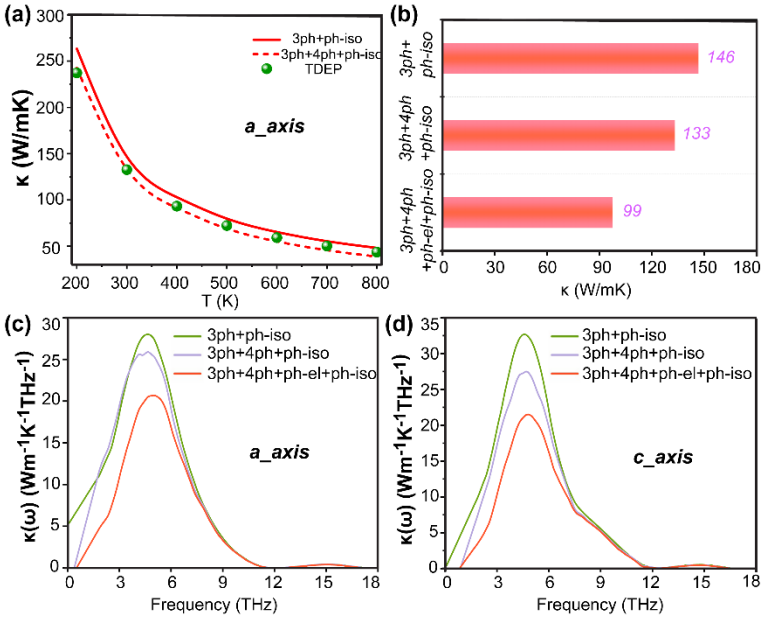

Fig. 3 (a) κ_{ph} of NbN vs temperature; (b) κ_{ph} under different scattering mechanisms; (c) and (d) are the differential of κ_{ph} to frequencies along the *a* and *c* axes, respectively.

4. The effect of pressure on lattice thermal conductivity (κ_{ph})

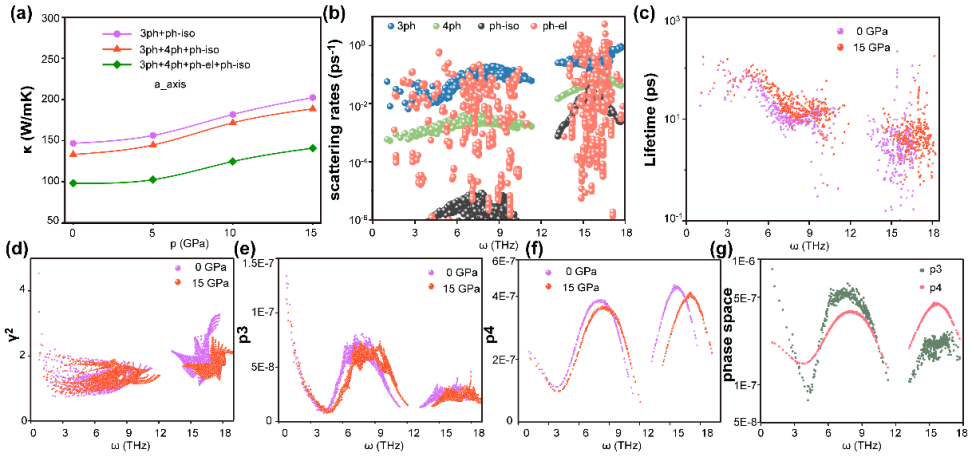

Fig. 4 (a) Effect of pressure on κ_{ph}; (b) scattering rates; (c) phonon relaxation time; (d) squared Gruneisen parameter (γ); (e) 3ph scattering phase space (P3), (f) 4ph scattering phase space (P4); (g) the comparison of P3 and P4.

As an effective approach of modulating the properties of materials, the κ of different materials changes differently with the increase of pressure. Much literature[10] has studied the change of NbN spatial phase with increasing

pressure, but no literature has calculated the change of κ under pressure and the micromechanics. Fig. 4(a) shows the increase of κ_{ph} under different scattering mechanisms from 0 GPa to 15 GPa. The decrease in κ_{ph} is greater when ep scattering is considered than when 4ph scattering is considered. To clarify the scattering mechanism of this material, we give the scattering rates of NbN, as shown in Fig. 4(b). In this figure, we can see that the ep scattering rate is close to the 3ph scattering rate over the whole frequency. Although ep scattering is strong in the high-frequency part, it is not in the frequency range that makes a decisive contribution to κ_{ph}. Unlike TaN[1] , the 4ph scattering of NbN has little effect on κ_{ph}. It can also be concluded from Fig. 4(b) that the 4ph scattering rate is always 1-2 orders of magnitude smaller than the 3ph scattering rate. For this reason, we give the P3 and P4 in Fig. 4(g), in the range of 0-12 THz, except that the P4 in 4-5 THz is greater than the P3, and the P3 is higher than the P4 in rest frequency. In the low-frequency, we compare the dispersion relationship between NbN and TaN and find that the highest frequency of the acoustic branch of NbN reaches about 11 THz, while TaN is 8 THz, which causes NbN 3ph scattering to be strong enough to weaken 4ph scattering. In Fig. 5, we give the 3ph and 4ph scattering rates, where the absorption process of 3ph scattering is dominant in 0-11 THz, and the 3ph scattering emission process is dominant in the high-frequency. The 4ph reforming process with the highest scattering rate in 4ph scattering, but is still lower than the 3ph scattering rates.

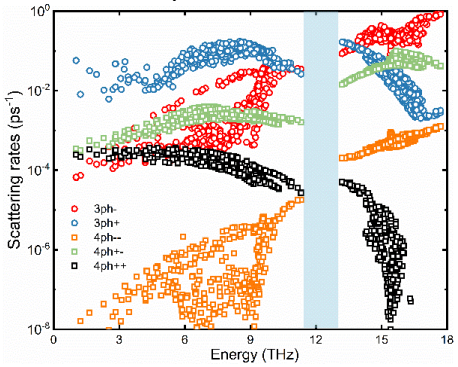

Fig. 5 Scattering rates of 3ph and 4ph scattering processes.

According to lattice dynamics theory, the κ_{ph} is mainly affected by specific heat capacity, group velocity and relaxation time. With the increase of pressure, the specific heat capacity and group velocity change weakly, so we focus on the analysis of phonon relaxation time. From Fig. 4(c), the phonon relaxation time of 15 GPa in low and mid frequencies is significantly higher than that of 0 GPa. The factors affecting phonon relaxation time are the γ and phonon scattering phase space. As mentioned in the previous chapter, the main contribution to κ_{ph} is frequencies in 3-9 THz, so we mainly focus on parameters in this range. For the γ, Fig. 4(d) shows no difference between the low and mid frequencies. However, from Fig. 4(e) and (f), the P3 and P4 at 15 GPa are lower than those at 0 GPa. Therefore, the scattering phase space is an important factor affecting the change of phonon relaxation time under pressure.

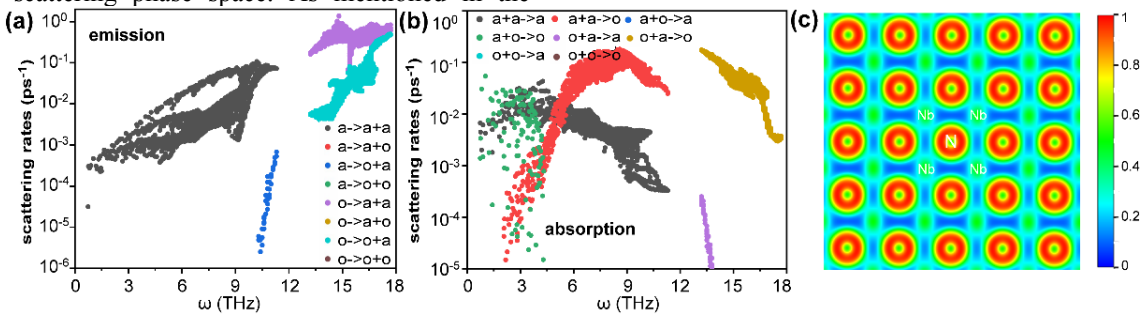

Fig. 6 The proportion of each channel during (a) the emission process and (b) the absorption process of 3ph scattering; (c) the electronic local function of NbN.

To further explore the scattering process, we give the scattering rates of eight channels of the 3ph scattering absorption and emission process. For the emission process, in the range of 0-9 THz, the scattering process is $a \to a + a$. For the absorption process, in the 0-6 THz, the scattering rate is mainly influenced by $a + o \to o$ and $a + a \to a$; in the range of 6-12 THz, the scattering process $a + a \to o$ is dominant. After analysis, it was found that most of the participants in the scattering process were acoustic phonons, which was directly related to the band gap in the phonon dispersion relationship. The existence of the band gap can exhibit bunching in the acoustic region, so that the conservation of momentum and energy is not satisfied, and then weaken part of the phonon scattering process. In addition, we give the electronic local function of NbN. Fig. 6 shows that N atoms are highly local, with strong covalent bonds between N and Nb.

5. phonon mean free path

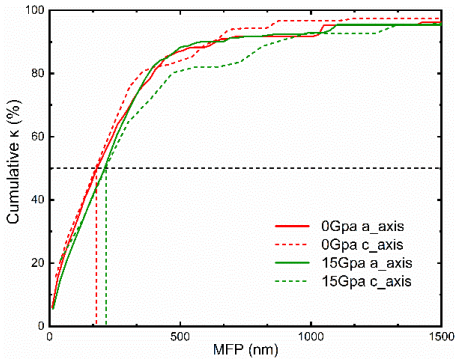

Fig. 7 Variation of cumulative κ_{ph} with phonon mean free path (MFP).

We give the variation of κ_{ph} with mean free path in Fig. 7. We can regulate the thermal transport properties by MFP. Here, we define the representative mean free path (RMFP) when 50% of the cumulative κ_{ph} is reached. When the nanostructure size is less than the RMFP, the corresponding phonon scattering channels increase, causing the κ_{ph} to decrease. Therefore, when designing micro-devices, the structure size should be larger than the RMFP of the corresponding material to avoid the decrease in κ. The RMFP of NbN at 0 GPa is 178 nm, which becomes 216 nm when the pressure increases to 15 GPa. Although the pressure can increase the RMFP of the material, the change is not significant. Moreover, the κ_{ph} of NbN is isotropic when the mean free path is less than RMFP.

6.Conclusions

In this work, the κ_{ph} of NbN is calculated by considering overall scattering mechanisms such as 3ph scattering, 4ph scattering, ep scattering, and iso scattering. We use the BTE and TDEP to calculate the κ_{ph}, and the data of the two are quite consistent at 300K. By analyzing the scattering rate of different scattering mechanisms, we find that the main scattering mechanisms affecting the κ_{ph} of NbN are 3ph scattering and ep scattering. Pressure is currently a common way to achieve superconductivity, we explore ways to improve the κ of materials by increasing pressure. As the pressure increases from 0 GPa to 15 GPa, the κ_{ph} increases by 148%, due to the increased phonon relaxation time which origins from the reduction in the scattering phase space. By considering the complete phonon scattering mechanism, we provide insights into the discovery of high κ materials and the regulation of κ.

Acknowledgments

This study was financially supported by the National Natural Science Foundation of China [52076031, 51720105007, 51806031], the Fundamental Research Funds for the Central Universities under Grant No. DUT19RC(3)006 and the computing resources from Super-computing Center of Dalian University of Technology are greatly acknowledged.

References

1. Kundu A, Yang X, Ma J, et al. (2021) Ultrahigh Thermal Conductivity of θ-Phase Tantalum Nitride. Physical Review Letters, 126(11): 115901.
2. Li X F, Du J Y. (2011) Theoretical Investigations on Mechanical Stability and Electronic Structure of NbN under Pressures. Applied Mechanics and Materials, 90–93: 1264–1271.
3. Yan R, Khalsa G, Vishwanath S, et al. (2018) GaN/NbN epitaxial semiconductor/superconductor heterostructures. Nature, 555(7695): 183–189.
4. Kresse G, Furthmüller J. (1996) Efficient iterative schemes for *ab initio* total-energy calculations using a plane-wave basis set. Physical Review B, 54(16): 11169–11186.
5. Li W, Carrete J, A. Katcho N, et al. (2014) ShengBTE: A solver of the Boltzmann transport equation for phonons. Computer Physics Communications, 185(6): 1747–1758.
6. Giannozzi P, Baroni S, Bonini N, et al. (2009) QUANTUM ESPRESSO: a modular and open-source software project for quantum simulations of materials. Journal of Physics: Condensed Matter, 21(39): 395502.
7. Poncé S, Margine E R, Verdi C, et al. (2016) EPW: Electron–phonon coupling, transport and superconducting properties using maximally localized Wannier functions. Computer Physics Communications, 209: 116–133.
8. Hellman O, Abrikosov I A. (2013) Temperature-dependent effective third-order interatomic force constants from first principles. Physical Review B, 88(14): 144301.
9. Blöchl P E. (1994) Projector augmented-wave method. Physical Review B, 50(24): 17953–17979.
10. Papaconstantopoulos D A, Pickett W E, Klein B M, et al. (1985) Electronic properties of transition-metal nitrides: The group-V and group-VI nitrides VN, NbN, TaN, CrN, MoN, and WN. Physical Review B, 31(2): 752–761.